Author Manuscript

Author Manuscript

Author Manuscript

Author Manuscript

HHS Public Access

Author manuscript

Nature. Author manuscript; available in PMC 2009 August 26.

Published in final edited form as:

Nature. 2009 February 26; 457(7233): 1133–1136. doi:10.1038/nature07658.

Intracortical circuits of pyramidal neurons reflect their long-range axonal targets

Solange P. Brown[1] and **Shaul Hestrin**[1]

[1]Department of Comparative Medicine, Stanford University School of Medicine, 300 Pasteur Drive, Edwards Building, R314, Stanford, California 94305-5342

Abstract

Cortical columns generate separate streams of information that are distributed to numerous cortical and subcortical brain regions1. We asked whether local intracortical circuits reflect these different processing streams by testing if the intracortical connectivity among pyramids reflects their long-range axonal targets. We recorded simultaneously from up to four retrogradely labelled pyramids that projected to the superior colliculus, the contralateral striatum or the contralateral cortex to assess their synaptic connectivity. Here we show that the probability of synaptic connection depends on the functional identity of both the presynaptic and postsynaptic neurons. We first found that the frequency of monosynaptic connections among corticostriatal pyramids is significantly higher than among corticocortical or corticotectal pyramids. We then show that the probability of feedforward connections from corticocortical neurons to corticotectal pyramids is approximately three- to fourfold higher than the probability of monosynaptic connections among corticocortical or corticotectal cells. Moreover, we found that the average axodendritic overlap of the presynaptic and postsynaptic pyramids could not fully explain the differences in connection probability that we observed. The selective synaptic interactions we describe demonstrate that the organization of local networks of pyramidal cells reflects the long-range targets of both the presynaptic and postsynaptic neurons.

The long-range axonal projections of cortical pyramidal neurons target unique sets of cortical and subcortical brain regions and define different functional classes of pyramids1. In addition, each pyramidal neuron elaborates extensive intracortical axon collaterals that generate the majority of excitatory input in neighbouring cortical neurons2–4. Recent work has shown that the probability of connection among pyramids is not homogeneous5–11. However, whether local synaptic interactions reflect the long-range axonal projections of both the presynaptic and the postsynaptic partner is not known.

Users may view, print, copy, and download text and data-mine the content in such documents, for the purposes of academic research, subject always to the full Conditions of use:http://www.nature.com/authors/editorial_policies/license.html#terms

Correspondence and requests for materials should be addressed to S.H. (shaul.hestrin@stanford.edu).

Author contributions: S.P.B. and S.H. designed the experiments. S.P.B. collected the data and S.P.B. and S.H. performed the analyses. S.P.B. and S.H. wrote the paper.

Full methods and any associated references are available in the online version of the paper at www.nature.com/nature.

Author information: Reprints and permissions information is available at www.nature.com/reprints.

The authors declare no competing financial interests

Author Manuscript Author Manuscript Author Manuscript Author Manuscript

Non-overlapping populations of pyramidal neurons projecting to different brain regions are intermingled within layer 5 (L5), the main output layer of the cortex1. We first compared the homotypic connectivity among L5 pyramids projecting to different brain regions. To address this question, we injected fluorescent latex microspheres into the ipsilateral superior colliculus to label corticotectal (CT) pyramids, the contralateral striatum to label corticostriatal (CS) neurons, or the contralateral visual cortex to label corticocortical (CC) pyramids. We next recorded in whole cell configuration from fluorescently labelled neurons and determined that the intrinsic physiological properties of CT, CS and CC pyramids were significantly different (Supplementary Fig. 1 and Supplementary Table 1), as expected for three distinct classes of pyramids12–14.

To assay the synaptic connectivity among pyramids projecting to the same long-range target, we recorded simultaneously from multiple fluorescently-labelled neurons using whole-cell patch clamp techniques. Action potentials were generated with brief current injections in each neuron in turn while recording the synaptic responses in the other neurons. In synaptically connected cells, these presynaptic action potentials elicited monosynaptic unitary excitatory postsynaptic potentials (EPSPs) in the postsynaptic partner. Monosynaptic connections were identified between neurons for all three cell types (Fig. 1a–c). The synaptic properties including the mean amplitudes and the paired-pulse ratio were similar among the three types of connections (Supplementary Table 2).

Although the properties of the synaptic responses were similar, the rate of monosynaptic connections among CS neurons was significantly higher than the rate among CT neurons or among CC neurons. Eighteen percent of CS→CS potential connections tested were monosynaptically connected (7/40 tested connections), a considerably higher connectivity than previously reported for L5 pyramids6, 10, 11, 15, 16. In contrast, only 7% of potential CT→CT connections (16/225 tested connections) and 5% of potential CC→CC connections (6/118 tested connections) were monosynaptically connected (Fig. 1d, $P = 0.034$, Pearson's chi-square test). Our results indicate that specific functional classes of pyramids can form highly interconnected networks embedded within the local circuitry of the cortex.

Several connectivity schemes could underlie the observed differences in the probability of connection among these cell types. First, the CT and CC cells we studied were located in the visual cortex whereas the CS cells were located in the sensorimotor cortex, raising the possibility of a regional effect on cortical connectivity. Second, each presynaptic cell type could connect to its neighbours with a characteristic frequency. CS neurons may simply connect to all their targets with a higher probability than CT or CC neurons. This interpretation is consistent with recent work showing that pyramids with different long-range projections have different probabilities of forming connections with neighbouring neurons10, 11, 17, suggesting that, rather than reflecting axonal target selectivity *per se*, the probability of connection is a global property specific to each pyramidal cell type. Third, cortical circuits may reflect the functional identity of the presynaptic and postsynaptic cell types. In this case, the intracortical connectivity among pyramids may reflect the long-range axonal projections of both the presynaptic and postsynaptic pyramids. Whether pyramids can synapse differentially onto neighbouring pyramids of different functional classes is not known.

Author Manuscript Author Manuscript Author Manuscript Author Manuscript

To differentiate among these possibilities, we targeted quadruplets composed of pyramids with two different long-range projections for electrophysiological recordings. This configuration allowed us to simultaneously compare the connectivity rates of two types of pyramids with two different postsynaptic targets. If the brain region or the functional identity of the presynaptic neuron dictates its connectivity with neighbouring pyramids, we would expect that a pyramid's probability of connection with the two different postsynaptic targets would be the same. However, if the probability of connection differs for the different types of connections, then intracortical connectivity depends on the functional identity of both the presynaptic and postsynaptic neuron.

We injected red fluorescent microspheres into the contralateral visual cortex and green fluorescent microspheres into the ipsilateral superior colliculus to label both CC and CT neurons in the same animal. We then recorded simultaneously from these classes of pyramidal neurons intermingled in layer 5 of the visual cortex and directly compared the probability of connection for four types of connections: CC→CC, CC→CT, CT→CT, and CT→CC (Figure 2a). We found that the probability of identifying CT→CC connections is 5% (4/86 connections tested), similar to the 7% probability of identifying a CT→CT connection ($P = 0.43$, Pearson's chi-square test), indicating that CT cells do not preferentially connect to CC as compared to CT pyramids. However, the probability of identifying a CC→CT connection is 19% (16/86 connections tested) whereas the probability of identifying a CC→CC connection is only 5% (Fig. 2b; $P = 0.002$, Pearson's chi-square test), indicating that CC pyramids preferentially target neighbouring CT neurons.

Our results indicate that the probability of identifying L5 pyramid-pyramid connections in visual cortex is not universally low. The probability of identifying CC→CT connections was as high as the probability of identifying CS→CS connections in the sensorimotor cortex. Second, our results indicate that the connectivity among pyramids is not simply a global characteristic of the presynaptic or the postsynaptic neuron. A CC axon is almost four times more likely to form a functional synapse with a local CT pyramid than with a CC pyramid, indicating that local intracortical circuits reflect the functional identity of the postsynaptic pyramid. Furthermore, the probability of identifying a monosynaptic connection is 19% for CC→CT combinations but only 7% for CT→CT combinations, indicating that the long-range target of the presynaptic cell is also important. Combined, our results suggest that it is the interplay between the functional identity of the presynaptic and the postsynaptic pyramid that determines the pattern of local microcircuits in the cortex.

Several authors have suggested that pyramids synapse probabilistically onto neighbouring neurons, and that their connectivity is a function of the average spatial overlap of their dendritic and axonal processes[4, 18–21]. If this is the case, the connectivity rates that we measured may simply reflect different average spatial overlaps for the five connections we tested rather than any local selection among different functional types of pyramidal neurons. To evaluate this possibility, we asked whether the frequency of monosynaptic connections we measured could be explained by differences in the distribution of the axonal and dendritic processes for these cell types. To address this question, we first reconstructed the three-dimensional morphology of L5 pyramids of each type filled with biocytin during our physiological recordings. The reconstructions of the dendritic and axonal arbours are shown

Author Manuscript Author Manuscript Author Manuscript Author Manuscript

in blue and red respectively (Fig. 3a–c). For each of the three cell types, the morphology of the L5 reconstructed neurons was similar11, 12, 22–24, indicating that the intracortical morphology of each functional class was consistent. However, the distribution of the dendritic and axonal processes among the three cells types was clearly different (Supplementary Fig. 2, Supplementary Fig 3 and Supplementary Fig 4).

Next, we asked whether these morphological differences could account for the differences in connectivity that we measured physiologically. To estimate the axodendritic overlap, we quantified the average local density of the dendritic and axonal processes for each cell by generating length density maps from the three-dimensional reconstructions for each type of process25. We then calculated the product of the axonal length density map and the dendritic length density map for each combination of neurons that we studied electrophysiologically (Fig. 3d). Figure 3d shows the results for neurons separated by 50 μm, the average distance between neurons in our physiological data set (see Methods Summary). Separating neurons from 0 to 200 μm, the largest distance between neurons in our data set, produced similar results. These axodendritic overlaps estimate the potential number of synapses formed between each combination of cell types studied. To determine whether the differences in axodendritic overlap could account for the functional connectivity that we measured, we next integrated the maps of axodendritic overlap to obtain the overall axodendritic overlap for each type of synaptic connection. The probability of connection and the axodendritic overlap for each of the cell combinations tested are plotted in Figure 3e. If a doubling in axodendritic overlap results in a doubling in the probability of connection, then the ratio of the axodendritic overlaps for two types of cell pairs should be equal to the ratio of their probabilities of connection. However, the ratio of connection probabilities for CC→CT connections and CC→CC connections, for example, was 3.7 while the ratio of axodendritic overlaps was 1.6. The resulting ratio of these two numbers was significantly greater than one ($P = 0.03$). Previous work has shown that synapses among neighbouring L5 pyramids are largely located on the proximal dendrites10, 11, 15, 26. Restricting our analyses to the perisomatic dendrites produced similar results ($P = 0.02$). Taken together, our data preclude a straightforward linear relationship between the average axodendritic overlap and the probability of connection and suggest that the average local density of axons and dendrites alone cannot explain the differences in the probability of connection.

Previous experiments have suggested that pyramids within L5 form a sparsely connected network, with probabilities of connection ranging from 1 – 12%6, 10, 11, 15, 16. Here, we show that the probability of identifying monosynaptic connections among CS pyramids and feedforward connections from CC to CT pyramids is approximately 20% per connection tested (equivalent to ~30–40% per pair tested). The excitatory monosynaptic connections among CS pyramids we describe could amplify the activation of interconnected ensembles of CS neurons, and the resulting coherent activity could depolarize functionally related striatal neurons consistent with the hypothesis that the activity of many converging CS axons is required to depolarize postsynaptic striatal neurons27, 28. We show that, while CC neurons are monosynaptically interconnected at low rates as are CT neurons, the local intracortical axons of CC cells target CT neurons with high probability. Interestingly, *in vivo* experiments showed that CT cells were preferentially activated by callosal stimulation and

Author Manuscript Author Manuscript Author Manuscript Author Manuscript

suggested that feedforward CC input is important in generating the receptive field properties of CT neurons29, 30. Our results indicate that the probability of connection among specific functional classes of pyramids can be quite high and suggest that highly interconnected functional subnetworks are embedded within the local circuitry of L5.

How local cortical circuits generate the cortex's output remains an open question. Previous work has shown that the connectivity between two pyramids influences the synaptic input they receive, demonstrating the existence of interconnected subnetworks within the neocortex6, 8, 9. We demonstrate that connections among pyramids reflect the long-range outputs of both the presynaptic and postsynaptic pyramids. Our results suggest an approach for understanding the function of specialized subnetworks embedded within cortical circuits. Unravelling the local circuits of pyramidal neurons whose long-range targets are known will allow us to understand how the different cortical outputs are generated within the cortical microcircuit. Given the diversity in the distant targets of pyramidal neurons, our findings suggest the existence of multiple networks of pyramidal neurons whose local intracortical connections subserve the specific roles played by their long-range axons.

Methods Summary

Mice (P14 to P17) were anesthetized and fluorescently labelled latex microspheres (RetroBeads, Lumafluor, Naples, FL) were injected into the ipsilateral superior colliculus, the contralateral striatum and the contralateral cortex to retrogradely label cortical neurons projecting to each target. One or more days later, parasagittal cortical slices were sectioned. Neurons labelled with fluorescent beads were targeted for simultaneous whole cell patch clamp recordings and their synaptic connectivity was assessed (see Methods). The morphology of the recorded neurons was revealed with biocytin using standard techniques and was reconstructed in three dimensions. To estimate the spatial overlap of the axonal and dendritic processes of the presynaptic and postsynaptic cells, we determined the axonal and dendritic length density maps of each cell. The axonal length density map of each cell of the appropriate presynaptic cell type (either CT, CS, or CC) was multiplied by each dendritic length density map of each cell of the relevant postsynaptic cell type. Because the pairs of cells we studied were separated by an average of 53 ± 24 SD μm (n = 235 pairs; range: 10–200 μm), we shifted the dendritic length density map 50 μm relative to the axonal length density map to estimate the spatial overlap, and these results are compared with the measured physiological connectivity (Figure 3). Because the distance between pairs of recorded cells ranged from 10 to 200 μm, we also shifted the dendritic length density maps from 0 to 200 μm relative to the axonal length density maps. We performed similar analyses with the neurons aligned by their soma position. We also restricted the analysis to the perisomatic dendritic processes as this is where synapses among L5 pyramids are largely located10, 11, 15, 26. These manipulations all resulted in axodendritic overlaps similar to those shown in Figure 3 (data not shown).

Author Manuscript Author Manuscript Author Manuscript Author Manuscript

Methods

Neuronal labelling

All experimental procedures were approved by the Institutional Animal Care and Use Committee of Stanford University. Juvenile mice (P14 to P17; C57BL/6 × CD-1 and YFP H-line31), were anesthetized and placed in a stereotaxic frame. Using stereotaxic coordinates adjusted for the age of the mice32, two to 15 sites in the striatum, the superior colliculus and/or the contralateral cortex were injected with 50 nL of a suspension of fluorescently labelled latex microspheres33 (red or green RetroBeads, Lumafluor, Naples, FL). Buprenorphine (0.05 mg/kg) was administered to alleviate post-operative discomfort. Injections into the superior colliculus labelled neurons in layer 5 (L5) of the ipsilateral visual cortex. Injections into the striatum labelled neurons in layers 2/3 and 5 of ipsilateral and contralateral cortex. Only those cells in L5 of the cortex contralateral to the injection site, representing a subset of corticostriatal cells whose projections include the contralateral striatum, were targeted for further study34–36. When studying corticocortical (CC) connections, we always simultaneously labelled CC and corticotectal (CT) neurons by injecting one colour of beads in the contralateral visual cortex and the other colour in the ipsilateral superior colliculus. There was essentially no overlap between these two cell populations22, 23. Only those CC cells intermingled with retrogradely labelled CT pyramids in L5 were targeted for physiological study. To verify the stereotaxic coordinates of the injections, injected hemispheres were fixed, sectioned, and mounted for visualization (Vectashield, Vector Laboratories, Burlingame, CA).

Slice preparation and cell identification

One or more days following the injections, each mouse was anesthetized and decapitated in an ice-cold sucrose solution composed of (in mM): 75 sucrose, 76 NaCl, 25 $NaHCO_3$, 25 glucose, 2.5 KCl, 1.25 NaH_2PO_4, 7 $MgCl_2$, 0.5 $CaCl_2$, pH 7.4, 325 mOsm. Parasagittal cortical slices, 300 μm thick, were sectioned from the selected hemisphere glued on a ramp set at a 30 angle (Integraslice 7550 MM, Campden Instruments, LaFayette, IN), and were maintained in the same solution at 32–34°C for 30 minutes before being transferred to artificial cerebrospinal fluid composed of (in mM): 125 NaCl, 2.5 KCl, 1.25 NaH_2PO_4, 1 $MgSO_4$, 2 $CaCl_2$, 26 $NaHCO_3$, 20 glucose, 4 lactic acid, 2 pyruvic acid, and 0.4 ascorbic acid, pH 7.4, 325 mOsm, at room temperature. All solutions were continuously bubbled with 95% O_2 and 5% CO_2. Retrogradely labelled neurons were identified under epifluorescent illumination (Axioskop 2 FS Plus, 40x objective, NA: 0.8, Zeiss) and targeted for recording using infrared differential interference contrast video microscopy (Sensicam QE, Cooke Corporation).

Electrophysiological recordings

Glass electrodes (2–4 mΩ) were filled with an internal solution containing (in mM): 2.7 KCl, 120 potassium methylsulfate, 9 HEPES, 0.18 EGTA, 4 MgATP, 0.3 NaGTP, 20 phosphocreatine(Na), pH 7.3, 295 mOsm. Simultaneous whole-cell patch clamp recordings of the targeted pyramidal cells were obtained using two Multiclamp 700A patch amplifiers (Molecular Devices, Sunnyvale, CA) in current-clamp mode. All experiments were performed at 32–35°C. Results were not corrected for the liquid junction potential.

Author Manuscript Author Manuscript Author Manuscript Author Manuscript

Data acquisition and analysis

All data acquisition and analysis was performed using custom software written in Igor Pro (Wavemetrics, Lake Oswego, OR) or Matlab (Mathworks, Natick, MA). To compare the adaptation rate of the three cell types, we injected a 200 ms step of depolarizing current adjusted to elicit 6 to 13 action potentials. A line was fitted to the plot of interspike intervals (ISIs) for each cell (Supplementary Fig. 1d). The first two ISIs were omitted from the analysis because CT cells fired a burst at the start of the current injection. The slope was then divided by the mean ISI to generate an adaptation index for each cell. An adaptation index of 0 indicates no adaptation in the spike rate. A positive adaptation index indicates an adapting spike train whereas a negative adaptation index indicates a spike train with increasingly shorter ISIs. The sag was assessed by fitting a single exponential to the recovery from a hyperpolarizing current step.

Synaptic connectivity was typically assessed by averaging 25 or more traces with two presynaptic action potentials at 20 or 25 Hz and/or 12 presynaptic action potentials at 100 Hz. Each presynaptic action potential was generated by a 3 ms injection of current, and individual trials were separated by 10 s. The 555 potential connections were classified as connected or unconnected while blinded to the identity of the presynaptic and postsynaptic neurons. Recorded neurons were separated by less than 200 μm (mean distance: 53 ± 24 SD μm, n = 235 pairs). There was no significant difference in the distance between pairs of connected and pairs of unconnected neurons for all connection types tested (data not shown). A bias in the vertical position of CC and CT neurons could not account for the differences in connectivity observed. The vertical distance we measured was a positive number when the CC cell was above the CT cell and was negative when the CC cell was below the CT cell. The mean vertical distance averaged 1 ± 33 SD μm which is not significantly different from 0 ($P = 0.83$; n = 86). There was also no difference in the vertical arrangement of connected and unconnected CC→CT pairs ($P = 0.51$).

Morphologic reconstruction and analysis

To reveal the morphology of the recorded neurons, 0.25% w/v biocytin was included in the pipette recording solution of at least one of the pipettes. Following the physiologic recordings, the tissue was processed using standard techniques to visualize the neurons with diaminobenzidine. The axons and dendrites of well-stained neurons were reconstructed in three dimensions using a Neurolucida system (Microbrightfield, Williston, VT) and a 100x oil-immersion objective (Zeiss, NA: 1.4). No correction was made for tissue shrinkage.

To analyze the distribution of neuronal processes for each cell, we measured the total length of dendrite or axon for each 50 μm × 50 μm × 300 μm cuboid in a 60 × 40 grid using Neuroexplorer (Microbrightfield). All reconstructed processes were included in this volume. Results from individual cells were then aligned either by soma position or relative to the pial margin. To estimate the spatial overlap of the dendritic and axonal processes of CT, CS and CC pyramids, we multiplied each axonal length density map by each dendritic length density map for each combination of cell types tested physiologically to generate an estimate of the potential number of synapses formed between a pair of neurons. The results were used to compare the potential synaptic connectivity for each combination of cell pairs.

Author Manuscript Author Manuscript Author Manuscript Author Manuscript

Results are expressed as means and standard errors unless otherwise noted. The physiological and morphological properties of the three cells types were compared using one-way analysis of variance or the Kruskal-Wallis analysis of variance for multiple comparisons. When only two cell types were compared, the *t*-test was used. The probability of connection was assessed using the Pearson's chi-square test (two tailed). The relationship between the connectivity and the axodendritic overlap was also assessed using a bootstrap approach to test the null hypothesis that the connectivity and the dendritic overlap were linearly related with a slope of one. The P values ranged from 0.017 to 0.039 using this approach for all the different configurations tested. These configurations included aligning the cell pairs relative to the pial margin or the cell bodies, separating the cells pairs by up to 200 μm, the largest separation in our physiological data set, and including only the perisomatic dendrites in the analysis.

Supplementary Material

Refer to Web version on PubMed Central for supplementary material.

Acknowledgments

We thank J. Li and S. Pak for technical assistance. This work was supported by National Institutes of Health grants to S.P.B and to S.H.

References

1. Jones, EG. Cerebral Cortex. Peters, A.; Jones, EG., editors. New York: Plenum; 1984. p. 521-553.
2. Kisvarday ZF, et al. Synaptic targets of HRP-filled layer III pyramidal cells in the cat striate cortex. Exp Brain Res. 1986; 64:541–552. [PubMed: 3803491]
3. McGuire BA, Hornung JP, Gilbert CD, Wiesel TN. Patterns of synaptic input to layer 4 of cat striate cortex. J Neurosci. 1984; 4:3021–3033. [PubMed: 6502220]
4. Braitenberg, V.; Schuz, A. Cortex: Statistics and Geometry of Neuronal Connectivity. Berlin: Springer-Verlag; 1998.
5. Kozloski J, Hamzei-Sichani F, Yuste R. Stereotyped position of local synaptic targets in neocortex. Science. 2001; 293:868–872. [PubMed: 11486089]
6. Song S, Sjostrom PJ, Reigl M, Nelson S, Chklovskii DB. Highly nonrandom features of synaptic connectivity in local cortical circuits. PLoS Biol. 2005; 3:e68. [PubMed: 15737062]
7. Wang Y, et al. Heterogeneity in the pyramidal network of the medial prefrontal cortex. Nat Neurosci. 2006; 9:534–542. [PubMed: 16547512]
8. Kampa BM, Letzkus JJ, Stuart GJ. Cortical feed-forward networks for binding different streams of sensory information. Nat Neurosci. 2006; 9:1472–1473. [PubMed: 17099707]
9. Yoshimura Y, Dantzker JL, Callaway EM. Excitatory cortical neurons form fine-scale functional networks. Nature. 2005; 433:868–873. [PubMed: 15729343]
10. Le Be JV, Silberberg G, Wang Y, Markram H. Morphological, electrophysiological, and synaptic properties of corticocallosal pyramidal cells in the neonatal rat neocortex. Cereb Cortex. 2006
11. Morishima M, Kawaguchi Y. Recurrent connection patterns of corticostriatal pyramidal cells in frontal cortex. J Neurosci. 2006; 6:4394–4405. [PubMed: 16624959]
12. Kasper EM, Larkman AU, Lubke J, Blakemore C. Pyramidal neurons in layer 5 of the rat visual cortex. I. Correlation among cell morphology, intrinsic electrophysiological properties, and axon targets. J Comp Neurol. 1994; 339:459–474. [PubMed: 8144741]
13. Wang Z, McCormick DA. Control of firing mode of corticotectal and corticopontine layer V burst-generating neurons by norepinephrine, acetylcholine, and 1S,3R-ACPD. J Neurosci. 1993; 13:2199–2216. [PubMed: 8386756]

Author Manuscript Author Manuscript Author Manuscript Author Manuscript

14. Hattox AM, Nelson SB. Layer V neurons in mouse cortex projecting to different targets have distinct physiological properties. J Neurophysiol. 2007; 98:3330–3340. [PubMed: 17898147]
15. Markram H, Lubke J, Frotscher M, Roth A, Sakmann B. Physiology and anatomy of synaptic connections between thick tufted pyramidal neurones in the developing rat neocortex. J Physiol. 1997; 500(Pt 2):409–440. [PubMed: 9147328]
16. Thomson AM, Deuchars J, West DC. Large, deep layer pyramid-pyramid single axon EPSPs in slices of rat motor cortex display paired pulse and frequency-dependent depression, mediated presynaptically and self-facilitation, mediated postsynaptically. J Neurophysiol. 1993; 70:2354–2369. [PubMed: 8120587]
17. Mercer A, et al. Excitatory connections made by presynaptic cortico-cortical pyramidal cells in layer 6 of the neocortex. Cereb Cortex. 2005; 15:1485–1496. [PubMed: 15647524]
18. Hellwig B. A quantitative analysis of the local connectivity between pyramidal neurons in layers 2/3 of the rat visual cortex. Biol Cybern. 2000; 82:111–121. [PubMed: 10664098]
19. Binzegger T, Douglas RJ, Martin KA. A quantitative map of the circuit of cat primary visual cortex. J Neurosci. 2004; 24:8441–8453. [PubMed: 15456817]
20. Stepanyants A, Chklovskii DB. Neurogeometry and potential synaptic connectivity. Trends Neurosci. 2005; 28:387–394. [PubMed: 15935485]
21. Kalisman N, Silberberg G, Markram H. Deriving physical connectivity from neuronal morphology. Biol Cybern. 2003; 88:210–218. [PubMed: 12647228]
22. Hallman LE, Schofield BR, Lin CS. Dendritic morphology and axon collaterals of corticotectal, corticopontine, and callosal neurons in layer V of primary visual cortex of the hooded rat. J Comp Neurol. 1988; 272:149–160. [PubMed: 3385021]
23. Hubener M, Bolz J. Morphology of identified projection neurons in layer 5 of rat visual cortex. Neurosci Lett. 1988; 94:76–81. [PubMed: 2468117]
24. Larsen DD, Wickersham IR, Callaway EM. Retrograde tracing with recombinant rabies virus reveals correlations between projection targets and dendritic architecture in layer 5 of mouse barrel cortex. Front. Neural Circuits. 2008
25. Shepherd GM, Stepanyants A, Bureau I, Chklovskii D, Svoboda K. Geometric and functional organization of cortical circuits. Nat Neurosci. 2005; 8:782–790. [PubMed: 15880111]
26. Frick A, Feldmeyer D, Helmstaedter M, Sakmann B. Monosynaptic connections between pairs of L5A pyramidal neurons in columns of juvenile rat somatosensory cortex. Cereb Cortex. 2008; 18:397–406. [PubMed: 17548800]
27. Stern EA, Jaeger D, Wilson CJ. Membrane potential synchrony of simultaneously recorded striatal spiny neurons in vivo. Nature. 1998; 394:475–478. [PubMed: 9697769]
28. Douglas RJ, Koch C, Mahowald M, Martin KA, Suarez HH. Recurrent excitation in neocortical circuits. Science. 1995; 269:981–985. [PubMed: 7638624]
29. Swadlow HA. Efferent neurons and suspected interneurons in binocular visual cortex of the awake rabbit: receptive fields and binocular properties. J Neurophysiol. 1988; 59:1162–1187. [PubMed: 3373273]
30. Singer W, Tretter F, Cynader M. Organization of cat striate cortex: a correlation of receptive-field properties with afferent and efferent connections. J Neurophysiol. 1975; 38:1080–1098. [PubMed: 1177006]
31. Feng G, et al. Imaging neuronal subsets in transgenic mice expressing multiple spectral variants of GFP. Neuron. 2000; 28:41–51. [PubMed: 11086982]
32. Paxinos, G.; Fanklin, KBJ. The Mouse Brain in Stereotaxic Coordinates. San Diego: Academic Press; 2001.
33. Katz LC, Burkhalter A, Dreyer WJ. Fluorescent latex microspheres as a retrograde neuronal marker for in vivo and in vitro studies of visual cortex. Nature. 1984; 310:498–500. [PubMed: 6205278]
34. Wilson CJ. Morphology and synaptic connections of crossed corticostriatal neurons in the rat. J Comp Neurol. 1987; 263:567–580. [PubMed: 2822779]
35. Lei W, Jiao Y, Del Mar N, Reiner A. Evidence for differential cortical input to direct pathway versus indirect pathway striatal projection neurons in rats. J Neurosci. 2004; 24:8289–8299. [PubMed: 15385612]

Author Manuscript Author Manuscript Author Manuscript Author Manuscript

36. Reiner A, Jiao Y, Del Mar N, Laverghetta AV, Lei WL. Differential morphology of pyramidal tract-type and intratelencephalically projecting-type corticostriatal neurons and their intrastriatal terminals in rats. J Comp Neurol. 2003; 457:420–440. [PubMed: 12561080]

Author Manuscript Author Manuscript Author Manuscript Author Manuscript

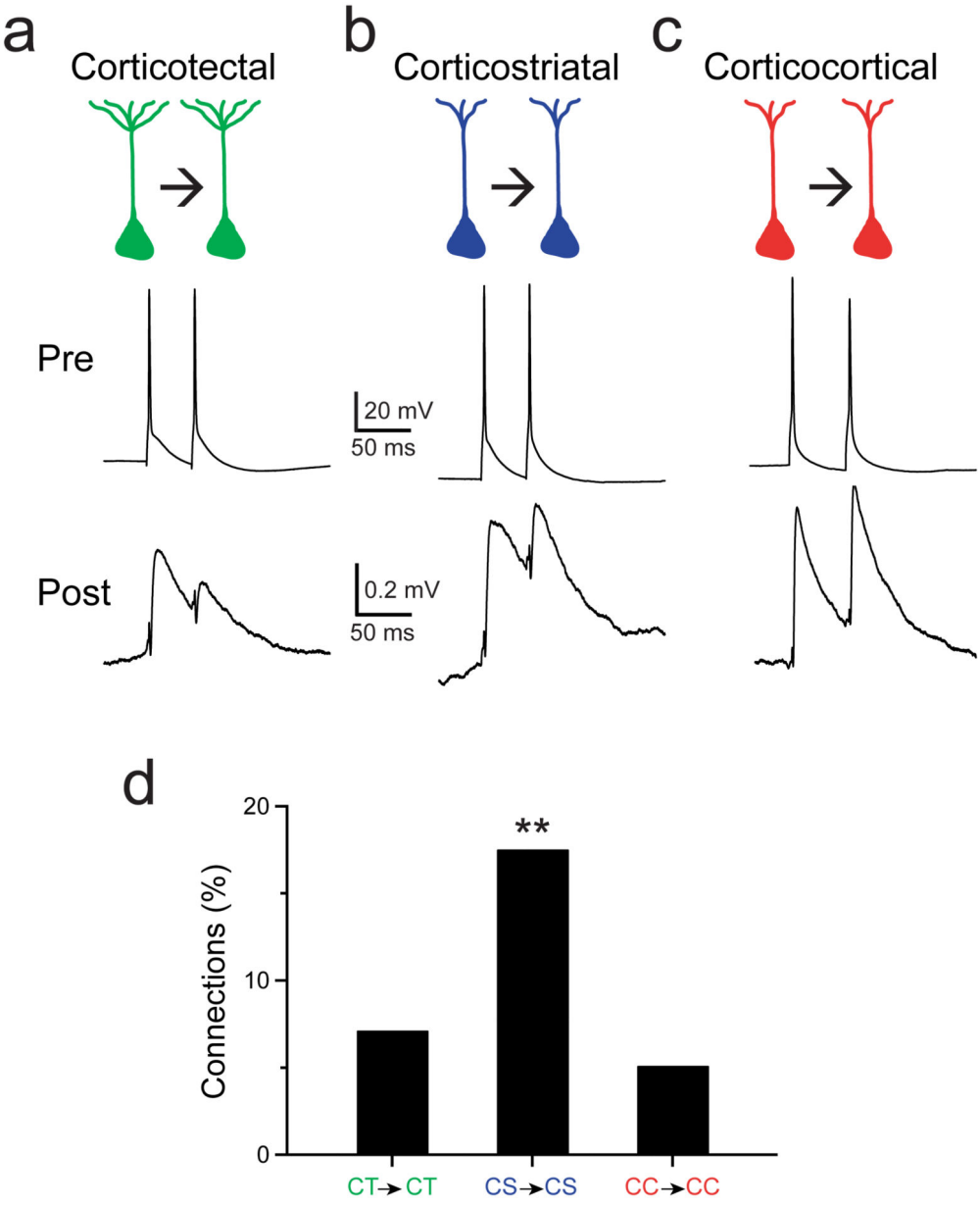

Figure 1.

Different frequencies of monosynaptic connections between corticotectal, corticostriatal or corticocortical neurons. Presynaptic action potentials elicit a synaptic response in a postsynaptic cell during simultaneous recordings from two monosynaptically-connected corticotectal neurons (**a**), corticostriatal neurons (**b**) and corticocortical neurons (**c**). **d,** The frequency of identified monosynaptic connections among connections tested is shown for corticotectal connections, corticostriatal connections and corticocortical connections; **P < 0.05.

Author Manuscript Author Manuscript Author Manuscript Author Manuscript

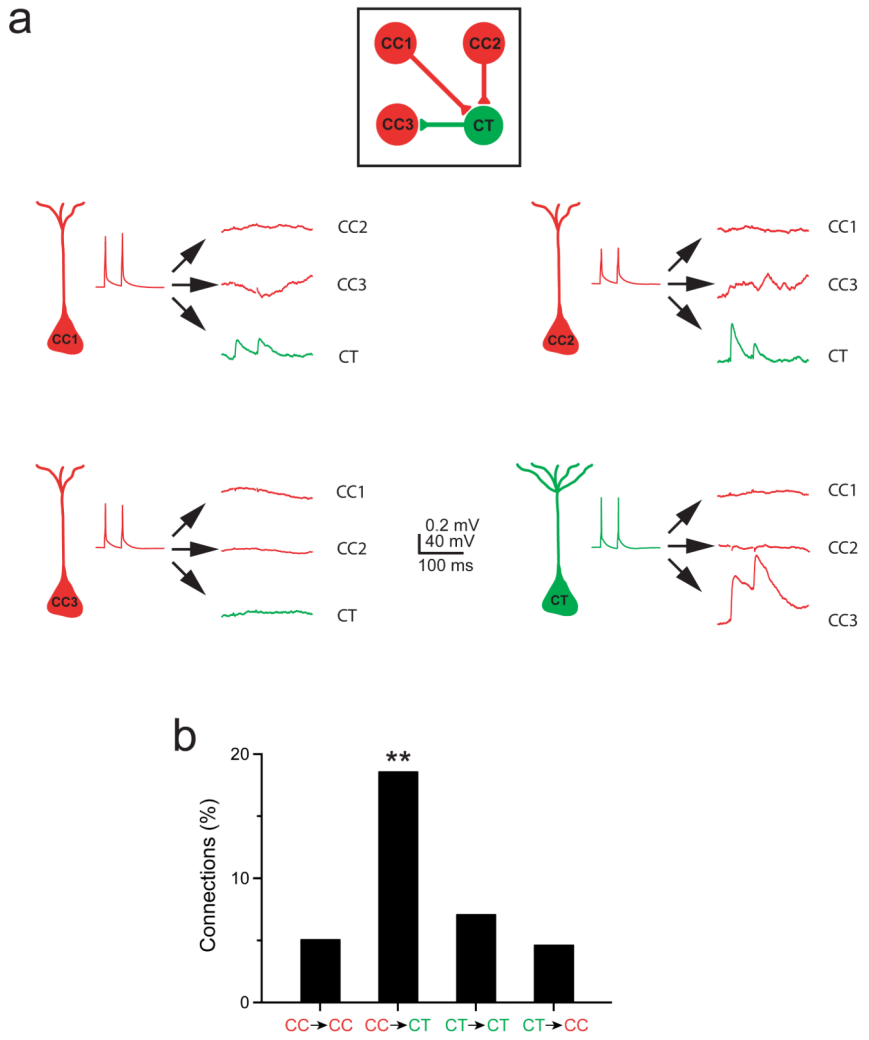

Figure 2.

Feedforward synaptic connections between presynaptic corticocortical neurons and neighbouring corticotectal neurons are almost four times more likely than connections among corticocortical neurons. **a,** An example of a quadruple recording. Three corticocortical neurons (red) and one corticotectal neuron (green) were recorded simultaneously and the 12 possible synaptic connections were tested. The corticocortical neurons, CC1 and CC2, synapsed onto the neighbouring corticotectal neuron. The corticotectal neuron in turn synapsed onto the corticocortical neuron, CC3. **b,** The frequency of synaptic connections identified among the tested connections is shown for the four possible types of connections among corticocortical and corticotectal neurons; **P < 0.01.

Author Manuscript Author Manuscript Author Manuscript Author Manuscript

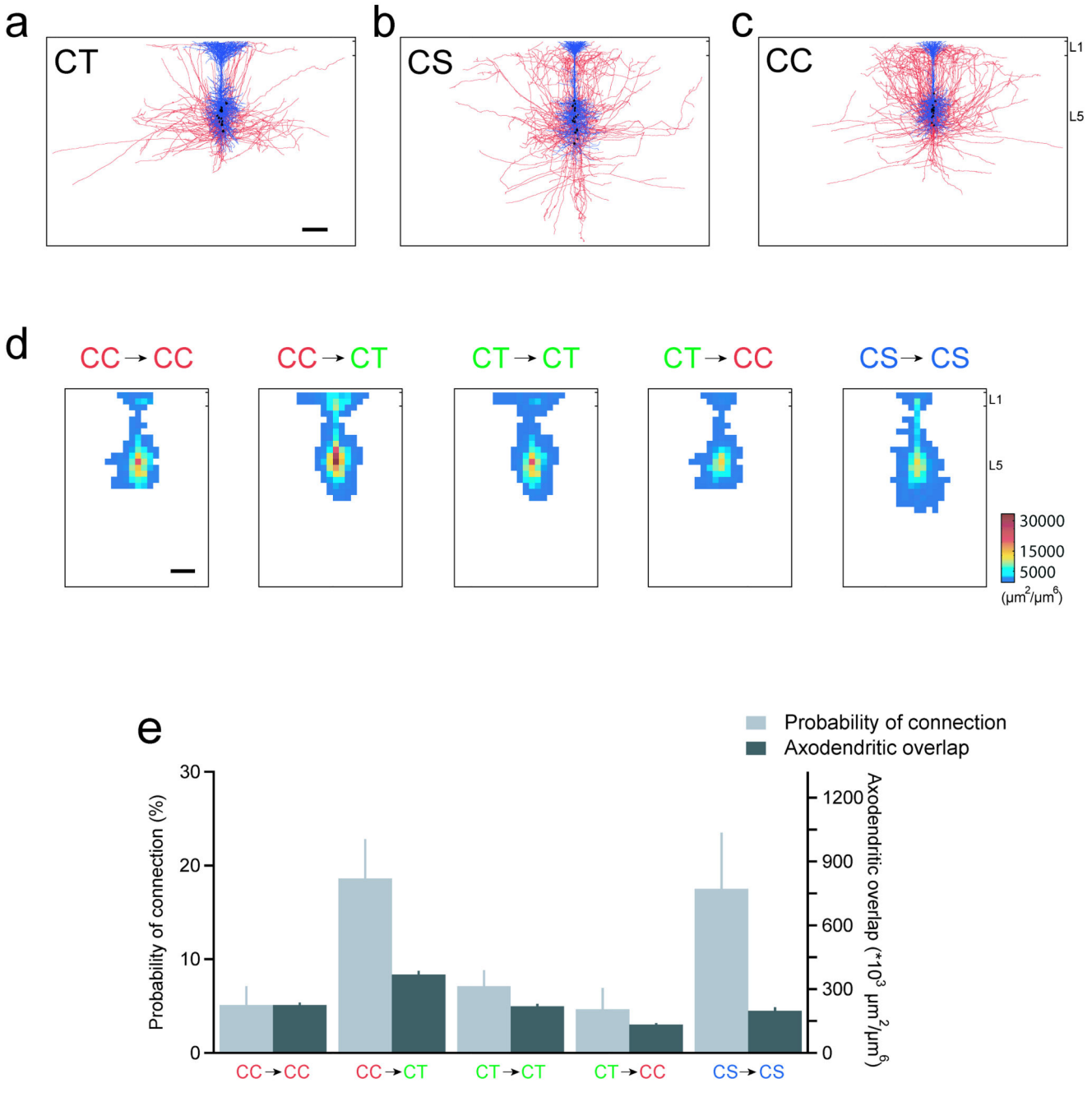

Figure 3.

The average axonal and dendritic architecture alone cannot explain differences in the connection probability. The morphology of 15 corticotectal (**a**), corticostriatal (**b**) and corticocortical neurons (**c**; blue: dendrites; red: axons; black: somas). **d,** The dendritic and axonal length-density maps were used to estimate the spatial overlap of the neuronal processes for the five types of connections tested physiologically. The resulting maps of axodendritic overlap, generated from cells aligned relative to the pial margin and shifted 50 μm relative to each other, are shown. Scale bars, 200 μm. **e,** The probability of physiological

connection and the average axodendritic overlap are plotted for each type of connection tested.

Author Manuscript Author Manuscript Author Manuscript Author Manuscript